HHS Public Access

Author manuscript

Cancer Res. Author manuscript; available in PMC 2019 October 04.

Published in final edited form as:

Cancer Res. 2019 May 01; 79(9): 2314–2326. doi:10.1158/0008-5472.CAN-18-3668.

Inhibition of miR-328–3p Impairs Cancer Stem Cell Function and Prevents Metastasis in Ovarian Cancer

Amit K. Srivastava[1], **Ananya Banerjee**[1,2], **Tiantian Cui**[1], **Chunhua Han**[1], **Shurui Cai**[1], **Lu Liu**[1,3], **Dayong Wu**[1], **Ri Cui**[4], **Zaibo Li**[5], **Xiaoli Zhang**[6], **Guozhen Xie**[1], **Karuppaiyah Selvendiran**[7], **Srinivas Patnaik**[2], **Adam R. Karpf**[8], **Jinsong Liu**[9], **David E. Cohn**[7], **Qi-En Wang**[1,10]

[1]Department of Radiation Oncology, College of Medicine, The Ohio State University, Columbus, Ohio.

[2]School of Biotechnology, KIIT Deemed to be University, Bhubaneswar, Odisha, India.

[3]Oncology Center, Zhujiang Hospital, Southern Medical University, Guangzhou, Guangdong, China.

[4]Department of Cancer Biology and Genetics, College of Medicine, The Ohio State University, Columbus, Ohio.

[5]Department of Pathology, College of Medicine, The Ohio State University, Columbus, Ohio.

[6]Center for Bioinformatics, College of Medicine, The Ohio State University, Columbus, Ohio.

[7]Department of Obstetrics and Gynecology, College of Medicine, The Ohio State University, Columbus, Ohio.

[8]Eppley Institute for Research in Cancer, Fred & Pamela Buffett Cancer Center, University of Nebraska Medical Center, Omaha, Nebraska.

[9]Department of Pathology, The University of Texas MD Anderson Cancer Center, Houston, Texas.

[10]Comprehensive Cancer Center, The Ohio State University, Columbus, Ohio.

Corresponding Author: Qi-En Wang, Ohio State University Wexner Medical Center, Room 1014, BRT, 460 W. 12th Avenue, Columbus, OH 43210. Phone: 614-292-9021; Fax: 614-292-9102; wang.771@osu.edu.

Current address for A.K. Srivastava: Cancer Biology & Inflammatory Disorder Division, Council of Scientific and Industrial Research-Indian Institute of Chemical Biology, Kolkata, West Bengal, India.

A.K. Srivastava, A. Banerjee, and T. Cui contributed equally to this article.

Authors' Contributions

Conception and design: A.K. Srivastava, A. Banerjee, D.E. Cohn, Q.-E. Wang

Development of methodology: A.K. Srivastava, A. Banerjee, T. Cui, C. Han, R. Cui

Acquisition of data (provided animals, acquired and managed patients, provided facilities, etc.): A.K. Srivastava, A. Banerjee, C. Han, S. Cai, K. Selvendiran, A.R. Karpf, J. Liu

Analysis and interpretation of data (e.g., statistical analysis, biostatistics, computational analysis): A.K. Srivastava, A. Banerjee, T. Cui, S. Cai, Z. Li, X. Zhang, G. Xie, D.E. Cohn, Q.-E. Wang

Writing, review, and/or revision of the manuscript: A.K. Srivastava, A. Banerjee, T. Cui, Z. Li, X. Zhang, G. Xie, A.R. Karpf, J. Liu, D.E. Cohn, Q.-E. Wang

Administrative, technical, or material support (i.e., reporting or organizing data, constructing databases): A. Banerjee, L. Liu, D. Wu, R. Cui, G. Xie

Study supervision: S. Patnaik, Q.-E. Wang

Note: Supplementary data for this article are available at Cancer Research Online (http://cancerres.aacrjournals.org/).

Disclosure of Potential Conflicts of Interest

No potential conflicts of interest were disclosed.

Abstract

Cancer stem cells (CSC) play a central role in cancer metastasis and development of drug resistance. miRNA are important in regulating CSC properties and are considered potential therapeutic targets. Here we report that miR-328–3p (miR-328) is significantly upregulated in ovarian CSC. High expression of miR-328 maintained CSC properties by directly targeting DNA damage binding protein 2, which has been shown previously to inhibit ovarian CSC. Reduced activity of ERK signaling in ovarian CSC, mainly due to a low level of reactive oxygen species, contributed to the enhanced expression of miR-328 and maintenance of CSC. Inhibition of miR-328 in mouse orthotopic ovarian xenografts impeded tumor growth and prevented tumor metastasis. In summary, our findings provide a novel mechanism underlying maintenance of the CSC population in ovarian cancer and suggest that targeted inhibition of miR-328 could be exploited for the eradication of CSC and aversion of tumor metastasis in ovarian cancer.

Significance: These findings present inhibition of miR-328 as a novel strategy for efficient elimination of CSC to prevent tumor metastasis and recurrence in patients with epithelial ovarian cancer.

Introduction

Tumor relapse and the development of therapeutic resistance are major factors leading to the high mortality of advanced cancer patients, but the underlying mechanisms have not yet been fully understood. The persistence of cancer stem cells (CSC) is well recognized to be responsible for treatment failure, tumor metastasis, and recurrence, mainly due to their enhanced tumorigenicity and chemoresistance. CSCs have been identified in a variety of solid tumors including epithelial ovarian cancer (EOC; refs. 1–3). Thus, eradication of CSCs could be an effective way to improve outcome of patients with EOC, and this requires us to understand how the CSC subpopulation is maintained.

CSCs possess characteristics of normal stem cells, particularly the ability of self-renewal and differentiation. In addition, CSCs also possess unique properties, such as high activity of aldehyde dehydrogenase (ALDH; ref. 4), ability to grow in suspension as spheres in the absence of serum (5), and extremely high tumorigenic potential (6). These CSC properties and the survival of CSCs can be maintained by a variety of pivotal factors and signaling pathways (7), which can be regulated by various epigenetic mechanisms, for example, histone modifications, DNA methylation, chromatin remodeling, and noncoding RNAs including miRNAs (8, 9).

Discoveries of miRNAs have provided a new avenue in understanding the regulatory mechanism of gene expression and epigenetic program. miRNAs typically function by base pairing with the 3′ untranslated regions (3′UTR) of their target mRNAs. The binding of a miRNA and its target mRNAs can result in translational inhibition, and/or mRNA destabilization, eventually leading to a change in the cellular protein level (10). miRNAs are involved in almost all biological processes, including the maintenance and differentiation of stem cells (11). More importantly, miRNAs have been reported to be differentially expressed in CSCs compared with their corresponding bulk cancer cells, and are considered an important epigenetic mechanism for regulating the properties of CSCs (8, 12). Therefore,

identification of dysregulated miRNAs in ovarian CSCs will be crucial for elucidating the mechanism underlying the maintenance of CSC properties, and then benefit to develop novel therapeutic methods to target and eliminate CSCs.

The ERK signaling pathway is one of four MAPK signaling pathways. The ERK cascade functions in cellular proliferation, differentiation, and survival, and its inappropriate activation is a common occurrence in human cancers (13). It has also been reported that ERK signaling plays a pivotal role in pluripotency maintenance. Suppressed ERK signaling is critical to the maintenance of self-renewal property of embryonic stem cells (ESC; refs. 14, 15), whereas enhanced ERK signaling promotes the differentiation of ESCs (16). However, it is unclear whether ERK signaling is also involved in the maintenance of the stem cell phenotype in CSCs.

In this study, we have revealed that miR-328–3p (termed miR-328) is highly expressed in ovarian CSCs, and plays a critical role in the maintenance of CSC properties as well as ovarian xenograft metastasis by directly downregulating DNA damage binding protein 2 (DDB2). In addition, we also found that high expression of miR-328 is due to a reduced activity of ERK signaling in ovarian CSCs caused by a low intracellular level of reactive oxygen species (ROS) in these cells.

Materials and Methods

Cell culture

Human ovarian cancer cell line Kuramochi was obtained from Japanese Collection of Research Bioresources Cell Bank, OVCAR4 was obtained from National Cancer Institute Division of Cancer Treatment and Diagnosis Cell Line Repository; the SKOV3 and OV2008 ovarian cancer cell lines were provided by Dr. Thomas C. Hamilton (Fox Chase Cancer Center), and Dr. Francois X. Claret (MD Anderson Cancer Center), respectively. All cell lines were authenticated by DNA (short tandem repeat) profiling and tested for mycoplasma contamination on January 22, 2019. These cells were maintained in RPMI1640 medium supplemented with 10% FBS, 100 μg/mL streptomycin, and 100 units/mL penicillin. To enrich CSCs, ovarian cancer cells were cultured in serum-free KnockOut DMEM/F12 medium supplemented with 20% KnockOut Serum Replacement, 20 ng/mL EGF, and 10 ng/mL bFGF (ThermoFisher Scientific) in Ultra-Low Attachment dishes (Corning) for at least 12 days.

microRNA expression assay

CSCs were enriched from Kuramochi and SKOV3 cells by culturing them under CSC culture conditions as described above. RNA was isolated from these sphere cultured CSCs along with adherently cultured bulk cancer cells using Norgen Total RNA Purification Kit (Norgen Biotek) following manufacturer's instructions. miRNA expression in these samples were analyzed in the OSUCCC Nucleic Acid Core Facility using the nCounter Human v3 miRNA Expression Assay Kit (Nanostring Technologies Inc.), which contains 800 human miRNAs. NanoString raw data were analyzed as described in Supplementary Methods and Materials. Data are deposited in Gene Expression Omnibus (GEO; GPL24289).

Isolation of primary tumor cells from patient-derived xenograft and freshly removed human ovarian tumors

A patient-derived xenograft (PDX; PDX-2414) was established by Dr. Jinsong Liu (MD Anderson Cancer Center, Houston, TX) from a patient with high-grade serous ovarian cancer (HGSOC) in accordance with a protocol approved by the MD Anderson Cancer Center's IRB, and was maintained in NOD/SCID mice. Freshly removed HGSOC tumors were obtained from Department of Pathology at the Ohio State University within 4 hours after surgery in accordance with a protocol approved by the Ohio State University's IRB. Written informed consents were obtained from all patients. Tumor cells were isolated, and putative CSCs were enriched as described in our previous work (17).

Plasmid, miRNA, gene transfection, and establishment of Tet On- or cumate-inducible stable cell lines

miR-328 mirVana mimic (miR-328-M) and inhibitor (miR-328-I), as well as negative control-miRNA (NC miR) were purchased from ThermoFisher Scientific. Cumate-inducible QM512B-MIZP328–3p plasmid was purchased from System Biosciences. shMIMIC Tet On-inducible miR-328 lentivirus was purchased from Dharmacon. pBabe-MEKDD plasmid was a gift of Dr. Ri Cui. MEKDD fragment was subcloned into the pCDH-CuO-MCS-IRES-GFP SparQ lentivector (SBI) to generate a cumate-inducible MEKDD expression vector. To construct wild-type psiCHECK-2-DDB2–3′-UTR, a 262-bp fragment of the 3′-UTR of the *DDB2* gene (position 1478–1740) that contains the putative miR-328 binding site was cloned into the psiCHECK-2 reporter vector (Promega) downstream of the Renilla luciferase gene (WT-DDB2). To construct mutant plasmids, the putative miR-328 binding site in *DDB2* 3′UTR was mutated (Mut-*DDB2*) using QuickChange Site-Directed Mutagenesis Kit (Stratagene). The insert was sequenced to verify the mutation.

miRNA and plasmids were transfected into cells using Lipofectamine 2000 (ThermoFisher Scientific). To establish a cell line with stably transfected Tet On-inducible miR-328 mimics (2008-shMIMIC-miR-328), OV2008 cells were infected with shMIMIC Tet On-inducible miR-328 lentivirus, selected in the medium containing 2 μg/mL puromycin, and the RFP-positive cells were sorted using fluorescence-activated cell sorting (FACS). To establish a cell line with stably transfected cumate-inducible anti-miR-328, OV2008 cells were transfected with cumate-inducible QM512B-MIZP328–3p plasmid, selected in the medium containing 2 μg/mL puromycin, and the RFP-positive cells were sorted using FACS. To establish a cell line with stably transfected cumate-inducible MEKDD expression, OV2008 cells were transfected with pCDH-CuO-MCS-IRES-GFP-MEKDD SparQ vector and pCDH-EF1α-T2A-Neo SparQ CymR expression vector (SBI) simultaneously, selected in the medium containing 500 μg/mL neomycin, and the GFP-positive cells after cumate treatment were sorted using FACS. The successful stable transfection was confirmed using either immunoblotting or qRT-PCR.

RNA isolation and qPCR analysis

Total RNA was extracted using TRIzol reagent (ThermoFisher Scientific), and the first strand cDNA was generated by the Reverse Transcription System (Promega) in a 20 μL reaction containing 1 μg of total RNA. A 0.5 μL aliquot of cDNA was amplified by Fast

SYBR Green PCR Master Mix (Applied Biosystems) in each 20 μL reaction. PCR reactions were run on the ABI 7900 Fast Real-Time PCR system (Applied Biosystems). The primers used for the real-time RT-PCR are listed in Supplementary Table S1. For miR-328 detection, TaqMan mature miR assays for miR-328 (Thermo-Fisher Scientific) was used to quantify the expression levels of miR-328, and TaqMan Pri-miRNA assay for pri-miR-328 (ThermoFisher Scientific) was used to quantify the expression level of pri-miR-328, according to the manufacture's protocols. RNU6B was used as a control.

Immunoblotting analyses

Whole-cell lysates were prepared by boiling cell pellets for 10 minutes in SDS lysis buffer [2% (w/v) SDS, 10% (v/v) glycerol, 62 mmol/L Tris·HCl, pH 6.8, and a complete miniprotease inhibitor mixture (Roche Applied Science)]. After protein quantification, equal amounts of proteins were loaded, separated on a polyacrylamide gel, and transferred to a nitrocellulose membrane. Protein bands were immuno-detected with various antibodies (Supplementary Table S2).

ALDH analyses

$ALDH^+$ cells were analyzed and sorted with the ALDEFLUOR Kit (STEMCELL Technologies) using flow cytometry. For each sample, one half of cells was treated with 50 mmol/L diethylaminobenzaldehyde (DEAB) to define negative gates.

Sphere-forming assay

A total of 1,000 cells were mixed with semisolid media (MethoCult H4100; STEMCELL Technologies) containing serum-free KnockOut DMEM/F12 medium supplemented with 20% KnockOut Serum Replacement, 20 ng/mL EGF, and 10 ng/mL bFGF, and seeded in six-well Ultra-Low Attachment plates (Corning). Sphere formation was assessed 12 days after cell seeding. To evaluate the frequency of sphere-forming cells (SFCf), cells were plated in Ultra-Low Attachment 96-well plates in a limiting dilution manner (1, 5, 10, 20 cells/well) using FACS. Cells were cultured in the above-mentioned medium for 12 days. The number of wells containing spheres was counted, and the SFCf was calculated using the ELDA software (http://bioinf.wehi.edu.au/software/elda/index.html; ref. 18).

Luciferase reporter assay

A total of 2×10^5 of OV2008 cells were seeded in 12-well plates. After 24 hours, cells were cotransfected with 200 ng of psiCHECK-2-DDB2–3′-UTR vectors and 20 μmol/L of miR-328 mimics. Cells were harvested 48 hours after transfection. Firefly and Renilla luciferase activities were measured by the Dual-Luciferase Reporter Assay Kit (Promega) on a Veritas Microplate Luminometer (Turner Biosystems). Renilla luciferase activity was normalized to Firefly luciferase activity to evaluate the effect of miR-328 on the expression of Renilla luciferase.

Microarray analysis

OV2008 cells were transfected with either miR-328 mimics or NC-miR for 2 days. Total RNA were extracted using Norgen Total RNA Purification Kit (Norgen Biotek), and

processed for Affymetrix transcriptsome assay using GeneChip Human transcriptome array 2.0 (Affymetrix). Data were analyzed by using Affymetrix transcriptsome console software as we previously conducted (19), and deposited in GEO repository (GSE119297).

Xenograft tumor study

NOD/SCID and Athymic nude mice (6–8 weeks, female, 20–25 g body weight) were obtained from The Jackson Laboratory (Bar Harbor, ME). Animals' care was in accordance with institutional guidelines, and all studies were performed with approval of the Institutional Animal Care and Use Committee at the Ohio State University. To determine the frequency of tumor-initiating cells (TICf) using the limiting dilution assay, three cell doses (1×10^6, 1×10^5, 1×10^4) of each sample were injected subcutaneously into the axillas of NOD/SCID mice. Mice were monitored for up to 4 weeks post-injection, and the tumor number per group within this period was used to calculate the TICf using aforementioned ELDA software (18).

To generate orthotopic ovarian cancer xenograft, OV2008-MIZP328–3p cells (1×10^5) were injected into the ovarian bursa of Athymic nude mice. Mice were divided into two groups, injected with either PBS or cumate (1.5 mg/mouse, SBI) once every other day for 14 days. Tumor mass was first monitored by MRI. Mice were then euthanized; tumor sizes were measured using a caliper; the peritoneal cavity was macroscopically inspected, and metastasis nodules were counted. Tumor xenografts and disseminated nodules were removed and pathologically examined using hematoxylin and eosin (H&E) staining to determine the histological type. Tumor cells were isolated and subjected to TICf analysis as described above.

Statistical analysis

Descriptive statistics, that is, means ± SD, are shown on the figures. Two sample *t* tests or ANOVA were performed for data analysis for experiments with two groups or more than two groups' comparisons. Generalized linear model as described by Hu and Smyth (18) was used for the TICf analysis. Log-rank analysis was used to determine statistical significance of the Kaplan–Meier survival curve. For all statistical methods, $P < 0.05$ was considered statistically significant. All tests were two-sided.

Results

miR-328-3p is highly expressed in CSCs

We attempted to identify miRNAs that are differentially expressed in ovarian CSCs. Given that CSCs possess a capability to grow in suspension as spheres in the absence of serum, CSCs can be enriched in sphere culture under CSC culture conditions (5, 17, 20). Therefore, we grew two EOC cell lines Kuramochi and SKOV3 under sphere culture conditions to enrich CSCs (Fig. 1A). These sphere cultured cells have been shown to possess CSC properties (Supplementary Fig. S1; ref. 20). The miRNA expression profiles in these cancer stem-like cells (CSLC) were determined. We identified 12 upregulated and 5 downregulated miRNAs in CSLCs isolated from two cell lines, compared to their corresponding bulk cancer cells (Fig. 1B and C; Supplementary Table S3). Among these differentially expressed

miRNAs, miR-328–3p (termed miR-328) is the most upregulated, and the upregulation of miR-328 was confirmed in CSLCs isolated from four EOC cell lines, one PDX from a HGSOC patient, and seven primary HGSOC tumors using qRT-PCR (Fig. 1D and E). In addition, highly expressed miR-328 was also found in CSLCs derived from pancreatic cancer cells, glioblastoma cells, and lung cancer cells (Supplementary Fig. S2), indicating that highly expressed miR-328 could be critical to the maintenance of CSCs in general.

Highly expressed miR-328 is critical to maintenance of the ovarian CSC population

To investigate the role of miR-328 in maintenance of the CSC pool in EOC cells, we transfected EOC cell line OV2008 and OVCAR4 with miR-328-I and analyzed the CSC populations defined by high activity of ALDH (4, 20, 21), or enhanced sphere formation capability (5). Inhibition of miR-328 limited the $ALDH^+$ cell subpopulation (Fig. 2A), and reduced the sphere formation capacity of EOC cells (Fig. 2B). Inhibition of miR-328 could also decrease the percentage of $CD44^+CD117^+$ cells in OV2008 cells (Supplementary Fig. S3), which have been demonstrated to possess CSC properties (20). Additionally, we generated a stable cell line, in which, anti-miR-328 oligonucleotides are expressed under a cumate inducible promoter (2008-MIZP328–3p). The successfully induced expression of anti-miR328 oligos was evidenced by increased expression of its known target gene *ABCG2* (Fig. 2C; ref. 22). Similar to the transient transfection of miR-328-I, cumate treatment also reduced the sphere formation capacity of OV2008 cells (Fig. 2D). Furthermore, we also assessed the effect of miR-328 inhibition on the tumorigenicity of EOC cells reflected by the TICf, which was determined by xenotransplantation with the limited dilution assay. Cumate-treated cells had lower TICf than untreated cells (Fig. 2E). All these data indicate that cumate-induced miR-328 inhibition can reduce the CSC population in EOC cells. In contrast, transfection of miR-328-M into EOC monolayer cells expanded the $ALDH^+$ cell population, increased their sphere formation capability, and their tumorigenicity (Supplementary Fig. S4).

To specifically investigate the contribution of miR-328 to the maintenance of CSC properties, we enriched CSCs from the EOC cell line OV2008 and OVCAR4 using sphere culture, and transfected them with miR-328-I. miR-328 inhibition significantly reduced the expression levels of *Sox2*, *Nanog*, and *Oct4*, three stem cell-specific transcription factors (Fig. 2F). We then isolated CSLCs characterized by $CD44^+CD117^+$ from 2008-MIZP328–3p cells and treated them with cumate. Cumate-induced miR-328 inhibition also significantly reduced the expression level of *Sox2*, *Nanog*, and *Oct4* (Fig. 2G). It is noteworthy that cumate treatment itself did not affect the expression of stem cell-specific genes (Supplementary Fig. S5). Thus, the effects of cumate treatment on CSLCs are caused by cumate-induced miR-328 inhibition. Furthermore, we assessed the sphere formation capacity of these cells by determining the SFCf in these cells with a limited dilution assay. We found that cumate-treated CSLCs showed a lower SFCf than untreated cells (Fig. 2H). Taken together, all these data indicate that miR-328 is critical to maintaining the CSC properties in EOC cells.

DDB2 is a direct target of miR-328 and mediates the function of miR-328 in the regulation of CSC properties

To identify the target genes of miR-328 through which miR-328 promotes the maintenance of CSC properties, we overexpressed miR-328 in the OV2008 EOC cell line, and profiled the downregulated genes. Fifty-one genes were found to be downregulated by miR-328 (>2 folds, $P < 0.01$; Fig. 3A; Supplementary Table S4). Among them, we are specifically interested in DDB2, because our previous study has demonstrated that DDB2 is able to reduce the abundance of CSCs in the bulk EOC cells (20). Sequence alignment showed that the *DDB2* gene possesses potential miR-328 binding sequence in its 3′UTR region (Fig. 3B). We further confirmed the direct binding of miR-328 to the 3′UTR of *DDB2* mRNA using the luciferase reporter assay (Fig. 3C and D), and validated the downregulation of DDB2 by miR-328 in a panel of EOC cell lines (Fig. 3E). To determine whether downregulated DDB2 is responsible for miR-328-mediated maintenance of the CSC population, we used cumate to induce the expression of anti-miR-328 oligos in CSCs derived from 2008-MIZP-328–3p cells. Meanwhile, these cells were transfected with DDB2 siRNA to counteract anti-miR-328-induced enhanced expression of DDB2 (Fig. 3F). As expected, cumate-induced anti-miR-328 reduced the sphere formation capacity of these cells, whereas simultaneous downregulation of DDB2 can restore their sphere formation capacity (Fig. 3G). These data indicate that highly expressed miR-328 in CSCs facilitates the maintenance of CSC properties by directly downregulating DDB2.

Reduced phosphorylation of ERK contributes to the upregulation of miR-328 in ovarian CSCs

It is reported that miR-328 expression can be downregulated by the ERK pathway activation in leukemia cells (23), and suppressed ERK signaling is critical to maintenance of the self-renewal property of ESCs (14, 15). Thus, we reasoned that CSCs must have a reduced ERK signaling activity, which help maintain a high level of miR-328. In support of this hypothesis, we found that ovarian CSLCs exhibited a markedly reduced phosphorylated ERK1/2 (p-ERK1/2) compared with their corresponding bulk cancer cells (Fig. 4A). CSLCs were cultured in serum-free media, and serum withdrawal can lead to decreased ERK activation (24). To exclude this possibility, we isolated CSLCs defined by $CD44^+CD117^+$ from the OV2008 cell line, and CSLCs defined by $CD133^+$ cells from the A549 cell line, and determined the p-ERK1/2 in these cells immediately. We again found a decreased p-ERK1/2 in the isolated CSLCs, which were cultured under the same condition as bulk cancer cells (Supplementary Fig. S6), indicating that CSCs indeed possess a relatively low activity of ERK signaling compared with their corresponding bulk cancer cells. To establish the relationship between the ERK activity and miR-328 expression in EOC cells, we treated a panel of EOC cell lines with the ERK inhibitor U0126 (Supplementary Fig. 7), and found that the miR-328 level was significantly increased (Fig. 4B). Vice versa, activation of the ERK pathway by overexpressing a constitutively activated MEK1 plasmid (MEKDD) in ovarian CSLCs dramatically reduced the expression of miR-328 (Fig. 4C and D). In addition, miR-328 levels in ovarian CSLCs can also be decreased by phorbol 12-myristate 13-acetate (PMA), an ERK activator (Supplementary Fig. S8; ref. 25). These data indicate that miR-328 expression can be negatively regulated by the ERK pathway activation in EOC cells. Furthermore, we found that ovarian CSCs possess an enhanced expression level of pri-

miR-328 compared with the bulk cancer cells. Inhibition of the ERK signaling in ovarian bulk cancer cells by U0126 significantly increased the pri-miR-328 expression, whereas activation of the ERK signaling by overexpressing constitutively activated MEK1 in ovarian CSLCs decreased the pri-miR-328 expression (Supplementary Fig. S9), indicating that the ERK signaling negatively regulates miR-328 expression, at least partially at the transcription level.

Inactivated ERK signaling facilitates the maintenance of CSC properties via upregulating miR-328

Given that suppressed ERK signaling is critical to maintaining ESCs (14, 15), and CSLCs possess reduced ERK signaling, we attempted to determine whether inactivated ERK signaling is required for the maintenance of CSC properties. We established a stable cell line in which MEKDD is expressed under a cumate inducible promoter (2008-SparQ-MEKDD), and enriched CSLCs from these cells using the sphere culture. Cumate treatment can successfully induce ERK1/2 phosphorylation (Fig. 4E) and reduce expression of stem cell specific genes, for example, *Oct4*, *Sox2*, and *Nanog*, in these CSLCs (Fig. 4F). In addition, cumate-induced ERK activation can also inhibit the sphere formation capacity and the tumorigenic potential of ovarian CSLCs (Supplementary Fig. S10). These data indicate that the reduced ERK activity plays a critical role in maintaining the stemness of CSCs.

In consideration of the fact that ERK inactivation increases miR-328 expression, and miR-328 promotes the maintenance of CSC properties, we hypothesized that inactivation of ERK signaling facilitates the maintenance of CSC traits by upregulating miR-328. To test this hypothesis, we isolated CSLCs from the 2008-SparQ-MEKDD cells, and activated the ERK signaling by treating them with cumate. Meanwhile, miR-328-M were transfected into these CSLCs to restore miR-328 that was depleted by ERK activation. Cumate treatment (ERK activation) can inhibit, whereas simultaneous transfection with miR-328-M restored CSLCs' sphere formation capacity (Fig. 4G). Besides MEKDD-induced ERK activation, we also used an ERK activator PMA to confirm this finding. PMA treatment, which increased ERK1/2 phosphorylation and decreased miR-328 expression, reduced the tumorigenic potential of both OV2008-CSLCs and OVCAR4-CSLCs (Supplementary Fig. S11). However, overexpression of miR-328 restored the tumorigenic potential that was inhibited by PMA in these cells (Supplementary Fig. S11). Taken together, these data indicate that ovarian CSLCs are characterized by reduced ERK signaling activity, which facilitates the maintenance of the CSC properties by upregulating miR-328.

Low intracellular ROS level contributes to the reduced activity of ERK signaling and enhanced expression of miR-328 in ovarian CSLCs

The ERK signaling is preferentially activated in response to growth factors. However, the ERK pathway can also be activated by ROS (26, 27), probably by activating growth factor receptors in the absence of the growth factor receptor ligands. In addition, oxidative stress was also reported to inhibit miR-328 expression in gastric cancer cells (28). Given that CSCs in a variety of tumors including ovarian cancer contain lower levels of ROS (Supplementary Fig. S12; refs. 29, 30), we reasoned that the reduced activity of ERK signaling and enhanced expression of miR-328 in CSCs can be attributed to the low intracellular ROS level. In

support of this hypothesis, we found that depletion of ROS by treatment with a ROS scavenger N-acetyl-L-cysteine can inhibit the phosphorylation of ERK1/2, and increase the expression level of miR-328 in ovarian cancer cells (Fig. 5A and B). Vice versa, treatment of ovarian CSCs with hydrogen peroxide (H_2O_2) enhanced phosphorylation of ERK1/2, and decreased the expression level of miR328 (Fig. 5C and D). More interestingly, inhibition of ERK signaling by treatment with U0126 can restore the miR-328 expression level that was reduced by H2O2 in ovarian CSLCs (Fig. 5E and F). These results indicate that the low level of ROS in CSLCs plays a critical role in sustaining a constitutively inactivated ERK signaling, which further maintains a highly expressed miR-328.

Although CSCs have a reduced level of ROS, its mechanisms in the maintenance of CSC properties are still unclear. Treatment of ovarian CSLCs with H_2O_2 can significantly reduce the expression of stem cell specific gene *Oct4* (Fig. 5G), as well as their sphere formation capability (Fig. 5H). Although simultaneous treatment with the ERK inhibitor U0126 can restore the *Oct4* expression level and SFCf in these H_2O_2-treated CSLCs (Fig. 5G and H), indicating that low level of H_2O_2 facilitates to maintain CSC properties by sustaining an inactivated ERK signaling, which ensures a highly expressed miR-328.

Inhibition of miR-328 impedes ovarian cancer growth and metastasis

Given that CSCs are believed to be responsible for tumor relapse and metastasis (31–33), we attempted to determine whether miR-328 inhibition can retard tumor growth and prevent tumor metastasis. 2008-MIZP328–3p cells were injected into the ovarian bursa of nude mice to generate orthotopic xenografts. Mice were administered with cumate to activate inhibition of miR-328 in xenograft cells. A markedly smaller tumor size was found in cumate-treated mice compared to PBS-treated mice (Fig. 6A; Supplementary Fig. S13). In addition, all PBS-treated mice (six mice) had ≥2 disseminated tumor nodules in peritoneal cavity, while only one of eight mice in cumate-treated group showed tumor nodules (Fig. 6B). H&E staining verified that the xenograft tumors from both PBS and cumate-treated mice, as well as the tumor nodules found in peritoneal cavity, had morphologic features of EOC (Fig. 6C). We further determined the TICf in xenograft cells. Cumate-induced miR-328 inhibition can dramatically reduce the TICf in xenografts (Fig. 6D and E). As a control, cumate itself did not affect tumor growth and peritoneal dissemination in mice bearing xenografts derived from OV2008 cells that do not possess cumate-inducible anti-miR-328 vectors (Supplementary Fig. S14). Taken together, these data indicate that inhibition of miR-328 is able to impede ovarian cancer growth and prevent metastasis by reducing the abundance of tumorigenic CSCs.

Overexpression of miR-328 is associated with worse outcome of patients with ovarian cancer

Given the oncogenic function of miR-328 in ovarian cancer, we sought to determine whether there is a relationship between the level of miR-328 expression and the prognosis in human patients with ovarian cancer. Korsunsky and colleagues have profiled miRNA expression in 19 EOC and 13 benign ovarian masses using TaqMan OpenArray (34). We reanalyzed these data (GSE81873) and found that the miR-328 level is higher in EOC than benign tissues (Supplementary Fig. S15). Kaplan–Meier survival curve showed that high miR-328

expression correlates with poor overall survival among patients with ovarian cancer (Supplementary Fig. S15). These analysis suggest that miR-328 could play an oncogenic role in the progression of ovarian cancer.

Discussion

miR-328 has been regarded as a cancer-related microRNA. Accumulating studies have suggested that it may play different roles as either an oncogene or a tumor suppressor depending on cancer type, indicating that the function of miR-328 could be tissue- and tumor-specific. In addition, low miR-328 expression has been linked to colorectal CSCs, because low miR-328 expression tends to correlate with the high side population (SP) fraction, which is believed to be a source of CSCs, indicating that the downregulated miR-328 expression may be favorable for the maintenance of CSCs in colorectal cancer (35). In contrast, data presented here showed that miR-328 is highly expressed in ovarian CSLCs, and plays critical roles in the maintenance of ovarian CSC properties, suggesting that overexpressed miR-328 could be favorable for CSC maintenance in ovarian cancer. Given that each miRNA could have multiple gene targets, and the regulation of these target gene expression by miRNA can be influenced by multiple factors including target-site accessibility (36), miR-328 could regulate CSC properties in different tumors by targeting different genes and pathways. Here, we showed that DDB2 is the key target gene of miR-328 in mediating miR-328-promoted maintenance of CSC properties in ovarian cancer.

DDB2 was first recognized as a DNA repair protein (37). Recently, new functions of DDB2 beyond its role in DNA repair have been identified, for example, enhancing cellular apoptosis (38–40); suppressing colon tumor metastasis through blocking epithelial–mesenchymal transition (EMT; ref. 41); and limiting the motility and invasiveness of invasive human breast tumor cells by regulating NF-κB activity (42), as well as mediating premature senescence (43). A correlation between low *DDB2* mRNA expression and poor outcome of patients with ovarian cancer and breast cancer has been established (20, 42). In addition, DDB2 has been shown to suppress the tumorigenicity of EOC cells (20) and colorectal cancer cells (41). DDB2 is also able to inhibit metastasis of colon cancer (41) and limit the invasiveness of breast cancer (42). Our previous study has demonstrated that DDB2 is able to reduce the abundance of CSCs in the bulk EOC cells, providing a novel mechanism to explain the DDB2-mediated suppression of tumorigenicity, and also suggesting that low expression of DDB2 is essential to maintaining CSCs (20, 44). We further demonstrated in the present study that downregulation of DDB2 is able to restore the self-renewal capacity that is reduced by miR-328 inhibition in ovarian CSCs. Given that DDB2 can directly inhibit the Wnt pathway (45), which plays an important role in upregulating the transcription of stem cell specific factors, for example, Oct4, Sox2, and Nanog (46), DDB2 must play a critical role in mediating miR-328-promoted maintenance of CSC properties via modulating the Wnt activity.

It has been reported that suppressed ERK signaling is critical to maintenance of the self-renewal property of ESCs (14, 15). Here, we further provide evidence showing that suppressed ERK signaling also contributes to maintenance of the self-renewal capacity of CSCs. Compared with the bulk cancer cells, CSCs possess a low activity of ERK signaling;

Forced activation of the ERK signaling compromises CSC properties and reduces the CSC abundance; while inhibition of the ERK activity expands the CSC population. Given that numerous tumors have activated ERK signaling (47), ERK signaling inhibitors have been developed for treatment of various cancers (48). However, the biggest challenge of ERK signaling inhibitors is that most patients relapse in less than a year (48). Our findings that the inactivated ERK signaling is important to the maintenance of CSC properties, suggest that ERK inhibitors-induced expansion of CSCs could be responsible for tumor relapse. Thus, it is warranted to develop new strategies to eliminate CSCs during ERK inhibitor treatment.

ERK signaling can regulate the cellular miR-328 level through multiple mechanisms. ERK is able to phosphorylate RNA-binding protein hnRNP-E2, promote its binding to the 5′UTR of *CEBPA* mRNA and inhibit C/EBPα expression (49). Given that C/EBPα can bind to miR-328 5′-flanking region directly to promote the transcription of miR-328, ERK-induced inhibition of C/EBPα expression can downregulate the transcription of pri-miR-328 (23, 50), which has also been found in this study.

ROS act as secondary messengers responsible for signal transduction to control gene expression. Normal stem cells and CSCs in a variety of tumors including ovarian cancer contain lower levels of ROS (29, 30). An important consequence of having a low ROS level in CSCs is the maintenance of stem cell properties (51, 52). However, it is still unclear how low ROS contributes to the maintenance of CSCs. Our findings in this study demonstrated that low ROS is critical to maintaining a high cellular level of miR-328 by sustaining a reduced ERK signaling. The cellular ERK signaling is not only activated in response to growth factors, such as EGF and PDGF, but also activated by cellular ROS (26, 27), probably by activating growth factor receptors without the growth factor ligands. It has been shown that ROS is able to activate the receptors of EGF and PDGF, which can further stimulate Ras and the subsequent activation of the ERK pathway (53, 54). Our data showed that scavenging ROS by antioxidants can reduce cellular ERK activation, further indicate that ROS plays an important role in sustaining an activated ERK signaling in cells. Therefore, given that ROS is critical to the activation of cellular ERK signaling, low ROS in CSCs could reduce the stimulation of the ERK pathway, and increase the cellular miR-328 level, which further promotes the maintenance of CSC characteristics by downregulating DDB2 (Fig. 6F).

In summary, we demonstrated that the ROS–ERK–miR-328–DDB2 axis plays a critical role in driving EOC progression by facilitating the maintenance of CSCs in tumors. Thus, inhibition of miR-328, or interruption of the ROS–ERK–miR-328–DDB2 axis can be exploited for the development of efficient strategies for eliminating CSCs to prevent ovarian tumor metastasis and recurrence, eventually leading to an improvement of the survival of patients with EOC.

Supplementary Material

Refer to Web version on PubMed Central for supplementary material.

Acknowledgments

We thank Dr. Thomas C. Hamilton (Fox Chase Cancer Center) and Dr. Francois X. Claret (University of Texas MD Anderson Cancer Center) for kindly providing ovarian cancer cell lines. This work was supported by grants from NIH (NCI R01CA211175), Phi Beta Psi Sorority, and OSUCCC Pelotonia Idea Award. A.K. Srivastava was a Pelotonia Postdoctoral Fellow.

The costs of publication of this article were defrayed in part by the payment of page charges. This article must therefore be hereby marked *advertisement* in accordance with 18 U.S.C. Section 1734 solely to indicate this fact.

References

1. Zhang S, Balch C, Chan MW, Lai HC, Matei D, Schilder JM, et al. Identification and characterization of ovarian cancer-initiating cells from primary human tumors. Cancer Res 2008;68:4311–20. [PubMed: 18519691]
2. Baba T, Convery PA, Matsumura N, Whitaker RS, Kondoh E, Perry T, et al. Epigenetic regulation of CD133 and tumorigenicity of CD133+ ovarian cancer cells. Oncogene 2009;28:209–18. [PubMed: 18836486]
3. Bapat SA, Mali AM, Koppikar CB, Kurrey NK. Stem and progenitor-like cells contribute to the aggressive behavior of human epithelial ovarian cancer. Cancer Res 2005;65:3025–9. [PubMed: 15833827]
4. Marcato P, Dean CA, Giacomantonio CA, Lee PW. Aldehyde dehydrogenase: its role as a cancer stem cell marker comes down to the specific isoform. Cell Cycle 2011;10:1378–84. [PubMed: 21552008]
5. Weiswald LB, Bellet D, Dangles-Marie V. Spherical cancer models in tumor biology. Neoplasia 2015;17:1–15. [PubMed: 25622895]
6. Clarke MF, Dick JE, Dirks PB, Eaves CJ, Jamieson CH, Jones DL, et al. Cancer stem cells–perspectives on current status and future directions: AACR Workshop on cancer stem cells. Cancer Res 2006;66:9339–44. [PubMed: 16990346]
7. Visvader JE, Lindeman GJ. Cancer stem cells: current status and evolving complexities. Cell Stem Cell 2012;10:717–28. [PubMed: 22704512]
8. Sun X, Jiao X, Pestell TG, Fan C, Qin S, Mirabelli E, et al. MicroRNAs and cancer stem cells: the sword and the shield. Oncogene 2014;33: 4967–77. [PubMed: 24240682]
9. Wainwright EN, Scaffidi P. Epigenetics and cancer stem cells: unleashing, hijacking, and restricting cellular plasticity. Trends Cancer 2017;3: 372–86. [PubMed: 28718414]
10. Fabian MR, Sonenberg N, Filipowicz W. Regulation of mRNA translation and stability by microRNAs. Annu Rev Biochem 2010;79:351–79. [PubMed: 20533884]
11. Gangaraju VK, Lin H. MicroRNAs: key regulators of stem cells. Nat Rev Mol Cell Biol 2009;10:116–25. [PubMed: 19165214]
12. Liu C, Tang DG. MicroRNA regulation of cancer stem cells. Cancer Res 2011;71:5950–4. [PubMed: 21917736]
13. Dhillon AS, Hagan S, Rath O, Kolch W. MAP kinase signalling pathways in cancer. Oncogene 2007;26:3279–90. [PubMed: 17496922]
14. Burdon T, Stracey C, Chambers I, Nichols J, Smith A. Suppression of SHP-2 and ERK signalling promotes self-renewal of mouse embryonic stem cells. Dev Biol 1999;210:30–43. [PubMed: 10364425]
15. Kim MO, Kim SH, Cho YY, Nadas J, Jeong CH, Yao K, et al. ERK1 and ERK2 regulate embryonic stem cell self-renewal through phosphorylation of Klf4. Nat Struct Mol Biol 2012;19:283–90. [PubMed: 22307056]
16. Lu CW, Yabuuchi A, Chen L, Viswanathan S, Kim K, Daley GQ. Ras-MAPK signaling promotes trophectoderm formation from embryonic stem cells and mouse embryos. Nat Genet 2008;40:921–6. [PubMed: 18536715]
17. Srivastava AK, Han C, Zhao R, Cui T, Dai Y, Mao H, et al. Enhanced expression of DNA polymerase eta contributes to cisplatin resistance of ovarian cancer stem cells. Proc Natl Acad Sci U S A 2015;112:4411–6. [PubMed: 25831546]

18. Hu Y, Smyth GK. ELDA: extreme limiting dilution analysis for comparing depleted and enriched populations in stem cell and other assays. J Immunol Methods 2009;347:70–8. [PubMed: 19567251]
19. Zhao R, Cui T, Han C, Zhang X, He J, Srivastava AK, et al. DDB2 modulates TGF-beta signal transduction in human ovarian cancer cells by downregulating NEDD4L. Nucleic Acids Res 2015;43:7838–49. [PubMed: 26130719]
20. Han C, Zhao R, Liu X, Srivastava A, Gong L, Mao H, et al. DDB2 suppresses tumorigenicity by limiting the cancer stem cell population in ovarian cancer. Mol Cancer Res 2014;12:784–94. [PubMed: 24574518]
21. Silva IA, Bai S, McLean K, Yang K, Griffith K, Thomas D, et al. Aldehyde dehydrogenase in combination with CD133 defines angiogenic ovarian cancer stem cells that portend poor patient survival. Cancer Res 2011;71: 3991–4001. [PubMed: 21498635]
22. Pan YZ, Morris ME, Yu AM. MicroRNA-328 negatively regulates the expression of breast cancer resistance protein (BCRP/ABCG2) in human cancer cells. Mol Pharmacol 2009;75:1374–9. [PubMed: 19270061]
23. Eiring AM, Harb JG, Neviani P, Garton C, Oaks JJ, Spizzo R, et al. miR-328 functions as an RNA decoy to modulate hnRNP E2 regulation of mRNA translation in leukemic blasts. Cell 2010;140:652–65. [PubMed: 20211135]
24. Ley R, Ewings KE, Hadfield K, Howes E, Balmanno K, Cook SJ. Extracellular signal-regulated kinases 1/2 are serum-stimulated “Bim(EL) kinases” that bind to the BH3-only protein Bim(EL) causing its phosphorylation and turnover. J Biol Chem 2004;279:8837–47. [PubMed: 14681225]
25. Besson A, Davy A, Robbins SM, Yong VW. Differential activation of ERKs to focal adhesions by PKC epsilon is required for PMA-induced adhesion and migration of human glioma cells. Oncogene 2001;20: 7398–407. [PubMed: 11704869]
26. Wu HW, Li HF, Wu XY, Zhao J, Guo J. Reactive oxygen species mediate ERK activation through different Raf-1-dependent signaling pathways following cerebral ischemia. Neurosci Lett 2008;432:83–7. [PubMed: 18243549]
27. Wang X, Liu JZ, Hu JX, Wu H, Li YL, Chen HL, et al. ROS-activated p38 MAPK/ERK-Akt cascade plays a central role in palmitic acid-stimulated hepatocyte proliferation. Free Radic Biol Med 2011;51:539–51. [PubMed: 21620957]
28. Ishimoto T, Sugihara H, Watanabe M, Sawayama H, Iwatsuki M, Baba Y, et al. Macrophage-derived reactive oxygen species suppress miR-328 targeting CD44 in cancer cells and promote redox adaptation. Carcinogenesis 2014;35:1003–11. [PubMed: 24318997]
29. Diehn M, Cho RW, Lobo NA, Kalisky T, Dorie MJ, Kulp AN, et al. Association of reactive oxygen species levels and radioresistance in cancer stem cells. Nature 2009;458:780–3. [PubMed: 19194462]
30. Pasto A, Bellio C, Pilotto G, Ciminale V, Silic-Benussi M, Guzzo G, et al. Cancer stem cells from epithelial ovarian cancer patients privilege oxidative phosphorylation, and resist glucose deprivation. Oncotarget 2014;5: 4305–19. [PubMed: 24946808]
31. Hermann PC, Huber SL, Heeschen C. Metastatic cancer stem cells: a new target for anti-cancer therapy? Cell Cycle 2008;7:188–93. [PubMed: 18256530]
32. Dean M, Fojo T, Bates S. Tumour stem cells and drug resistance. Nat Rev Cancer 2005;5:275–84. [PubMed: 15803154]
33. Nguyen LV, Vanner R, Dirks P, Eaves CJ. Cancer stem cells: an evolving concept. Nat Rev Cancer 2012;12:133–43. [PubMed: 22237392]
34. Korsunsky I, Parameswaran J, Shapira I, Lovecchio J, Menzin A, Whyte J, et al. Two microRNA signatures for malignancy and immune infiltration predict overall survival in advanced epithelial ovarian cancer. J Investig Med 2017;65:1068–76.
35. Xu XT, Xu Q, Tong JL, Zhu MM, Nie F, Chen X, et al. MicroRNA expression profiling identifies miR-328 regulates cancer stem cell-like SP cells in colorectal cancer. Br J Cancer 2012;106:1320–30. [PubMed: 22453125]
36. Kertesz M, Iovino N, Unnerstall U, Gaul U, Segal E. The role of site accessibility in microRNA target recognition. Nat Genet 2007;39:1278–84. [PubMed: 17893677]

37. Dualan R, Brody T, Keeney S, Nichols AF, Admon A, Linn S. Chromosomal localization and cDNA cloning of the genes (DDB1 and DDB2) for the p127 and p48 subunits of a human damage-specific DNA binding protein. Genomics 1995;29:62–9. [PubMed: 8530102]
38. Barakat BM, Wang QE, Han C, Milum K, Yin DT, Zhao Q, et al. Overexpression of DDB2 enhances the sensitivity of human ovarian cancer cells to cisplatin by augmenting cellular apoptosis. Int J Cancer 2009;127: 977–88.
39. Zhao R, Han C, Eisenhauer E, Kroger J, Zhao W, Yu J, et al. DNA damagebinding complex recruits HDAC1 to repress Bcl-2 transcription in human ovarian cancer cells. Mol Cancer Res 2014;12:370–80. [PubMed: 24249678]
40. Stoyanova T, Roy N, Kopanja D, Bagchi S, Raychaudhuri P. DDB2 decides cell fate following DNA damage. Proc Natl Acad Sci U S A 2009;106: 10690–5. [PubMed: 19541625]
41. Roy N, Bommi PV, Bhat UG, Bhattacharjee S, Elangovan I, Li J, et al. DDB2 suppresses epithelial-to-mesenchymal transition in colon cancer. Cancer Res 2013;73:3771–82. [PubMed: 23610444]
42. Ennen M, Klotz R, Touche N, Pinel S, Barbieux C, Besancenot V, et al. DDB2: a novel regulator of NF-kappaB and breast tumor invasion. Cancer Res 2013;73:5040–52. [PubMed: 23774208]
43. Roy N, Stoyanova T, Dominguez-Brauer C, Park HJ, Bagchi S, Raychaudhuri P. DDB2, an essential mediator of premature senescence. Mol Cell Biol 2010;30:2681–92. [PubMed: 20351176]
44. Cui T, Srivastava AK, Han C, Wu D, Wani N, Liu L, et al. DDB2 represses ovarian cancer cell dedifferentiation by suppressing ALDH1A1. Cell Death Dis 2018;9:561. [PubMed: 29752431]
45. Huang S, Fantini D, Merrill BJ, Bagchi S, Guzman G, Raychaudhuri P. DDB2 is a novel regulator of Wnt signaling in colon cancer. Cancer Res 2017;77:6562–75. [PubMed: 29021137]
46. Faunes F, Hayward P, Descalzo SM, Chatterjee SS, Balayo T, Trott J, et al. A membrane-associated beta-catenin/Oct4 complex correlates with ground-state pluripotency in mouse embryonic stem cells. Development 2013; 140:1171–83. [PubMed: 23444350]
47. Roberts PJ, Der CJ. Targeting the Raf-MEK-ERK mitogen-activated protein kinase cascade for the treatment of cancer. Oncogene 2007;26:3291–310. [PubMed: 17496923]
48. Samatar AA, Poulikakos PI. Targeting RAS-ERK signalling in cancer: promises and challenges. Nat Rev Drug Discov 2014;13:928–42. [PubMed: 25435214]
49. Chang JS, Santhanam R, Trotta R, Neviani P, Eiring AM, Briercheck E, et al. High levels of the BCR/ABL oncoprotein are required for the MAPK-hnRNP-E2 dependent suppression of C/EBPalpha-driven myeloid differentiation. Blood 2007;110:994–1003. [PubMed: 17475908]
50. Saito J, Hirota T, Furuta S, Kobayashi D, Takane H, Ieiri I. Association between DNA methylation in the miR-328 5'-flanking region and inter-individual differences in miR-328 and BCRP expression in human placenta. PLoS One 2013;8:e72906. [PubMed: 23991164]
51. Yuan S, Lu Y, Yang J, Chen G, Kim S, Feng L, et al. Metabolic activation of mitochondria in glioma stem cells promotes cancer development through a reactive oxygen species-mediated mechanism. Stem Cell Res Ther 2015;6: 198–212. [PubMed: 26472041]
52. Piskounova E, Agathocleous M, Murphy MM, Hu Z, Huddlestun SE, Zhao Z, et al. Oxidative stress inhibits distant metastasis by human melanoma cells. Nature 2015;527:186–91. [PubMed: 26466563]
53. Leon-Buitimea A, Rodriguez-Fragoso L, Lauer FT, Bowles H, Thompson TA, Burchiel SW. Ethanol-induced oxidative stress is associated with EGF receptor phosphorylation in MCF-10A cells overexpressing CYP2E1. Toxicol Lett 2012;209:161–5. [PubMed: 22222162]
54. Lei H, Kazlauskas A. Growth factors outside of the platelet-derived growth factor (PDGF) family employ reactive oxygen species/Src family kinases to activate PDGF receptor alpha and thereby promote proliferation and survival of cells. J Biol Chem 2009;284:6329–36. [PubMed: 19126548]

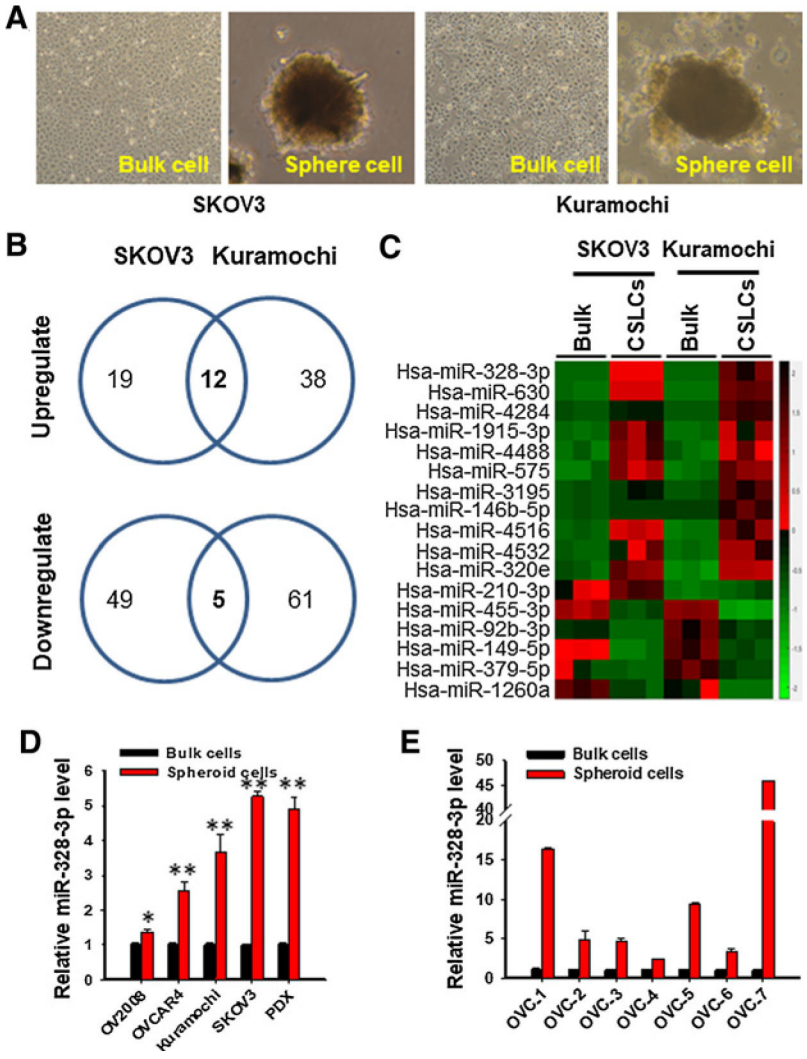

Figure 1.

Ovarian CSCs possess highly expressed miR-328. **A–C,** NanoString nCounter analysis revealed 12 upregulated and 5 downregulated miRNAs in spheroid cells compared with their corresponding bulk cancer cells. EOC cell lines Kuramochi and SKOV3 were cultured in Ultra-Low Attachment dishes with CSC culture medium as described in Materials and Methods for 12 days to enrich CSCs (**A**). The spheres formed under these culture conditions (CSLCs), as well as monolayer cells cultured under the regular culture conditions (bulk cells), were harvested; RNA was isolated and subjected to miRNA screening using NanoString nCounter. **B,** Venn diagram shows the number of altered miRNA in CSLCs derived from Kuramochi and SKOV3 cell lines. **C,** Heat map of altered miRNA in CSLCs derived from both cell lines was generated. **D,** Enhanced expression of miR-328 was confirmed in CSLCs isolated from four EOC cell lines and one PDX. Spheroid (CSLCs) and adherent (Bulk) cells were harvested from various EOC cell lines and one ovarian tumor PDX; miR-328 was quantified using qRT-PCR. $n = 3$; Bar, SD; *, $P < 0.05$; **, $P < 0.001$. **E,** Enhanced expression of miR-328 was confirmed in spheroid cells isolated from primary HGSOC samples. Tumor cells were isolated from seven freshly removed primary HGSOC

samples, cultured under sphere culture conditions (Spheroid) and adherent culture conditions (Bulk). The miR-328 level was quantified using qRT-PCR. $n = 3$; bar, SD. Analysis by the linear mixed model indicates that miR-328 expression increased significantly in spheroid cells compared with bulk cancer cells ($P < 0.0001$).

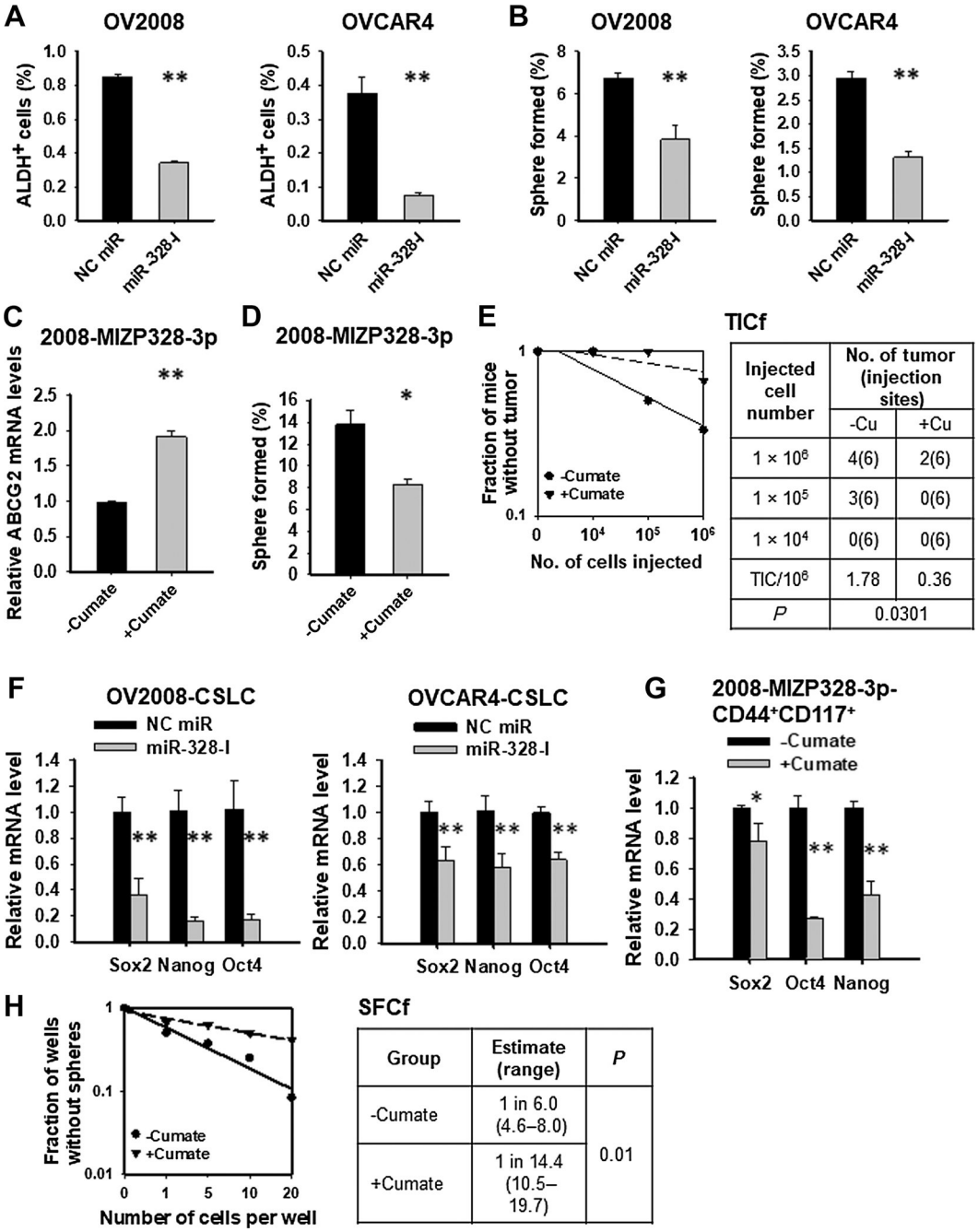

Figure 2.

miR-328 is critical to maintaining the CSC population in EOC cells. **A,** Inhibition of miR-328 (miR-328-I) decreased the abundance of ALDH$^+$ cells in various EOC cell lines. OV2008 and OVCAR4 cells were transiently transfected with either NC miR or miR-328-I for 48 hours. The proportion of ALDH$^+$ cells was analyzed with ALDEFLUOR assay using FACS. $N = 3$; bar, SD. **B,** Inhibition of miR-328 reduced the sphere formation capability of EOC cell lines. OV2008 and OVCAR4 cells were transiently transfected with either NC miR or miR-328-I for 48 hours. Semisolid colony formation assay was used to determine their sphere formation capacity. $N = 3$; bar, SD. **C–E,** Inhibition of miR-328 reduced the

tumorigenic potential of the EOC cells. OV2008 cells possessing cumate-inducible anti-miR-328 expression vectors (2008-MIZP328–3p) were treated with or without cumate for 3 days. The expression level of *ABCG2* (a direct target of miR-328) was determined to assess the inhibition of miR-328 (**C**). Semisolid colony formation assay was used to determine their sphere formation capacity (**D**). Xenotransplantation limiting dilution assay was used to estimate the TICf (**E**). $N = 3$; bar, SD. **F–H,** Inhibition of miR-328 in ovarian CSLCs reduces the CSC properties. CSLCs were isolated from OV2008 and OVCAR4 cells, transfected with either NC miR or miR-328-I for 48 hours, and the expression of stem cell–specific genes was determined using qRT-PCR (**F**). CSLCs were isolated from 2008-MIZP328–3p cells, treated with or without cumate for 3 days. The expression of stem cell–specific genes was determined (**G**). Cells were plated in a limiting dilution manner in 96-well Ultra-Low Attachment plates with CSC culture medium, and the number of wells containing spheres was calculated after 12 days to calculate the SFCf (**H**). $N = 3$; bar, SD; *, $P < 0.05$; **, $P < 0.01$.

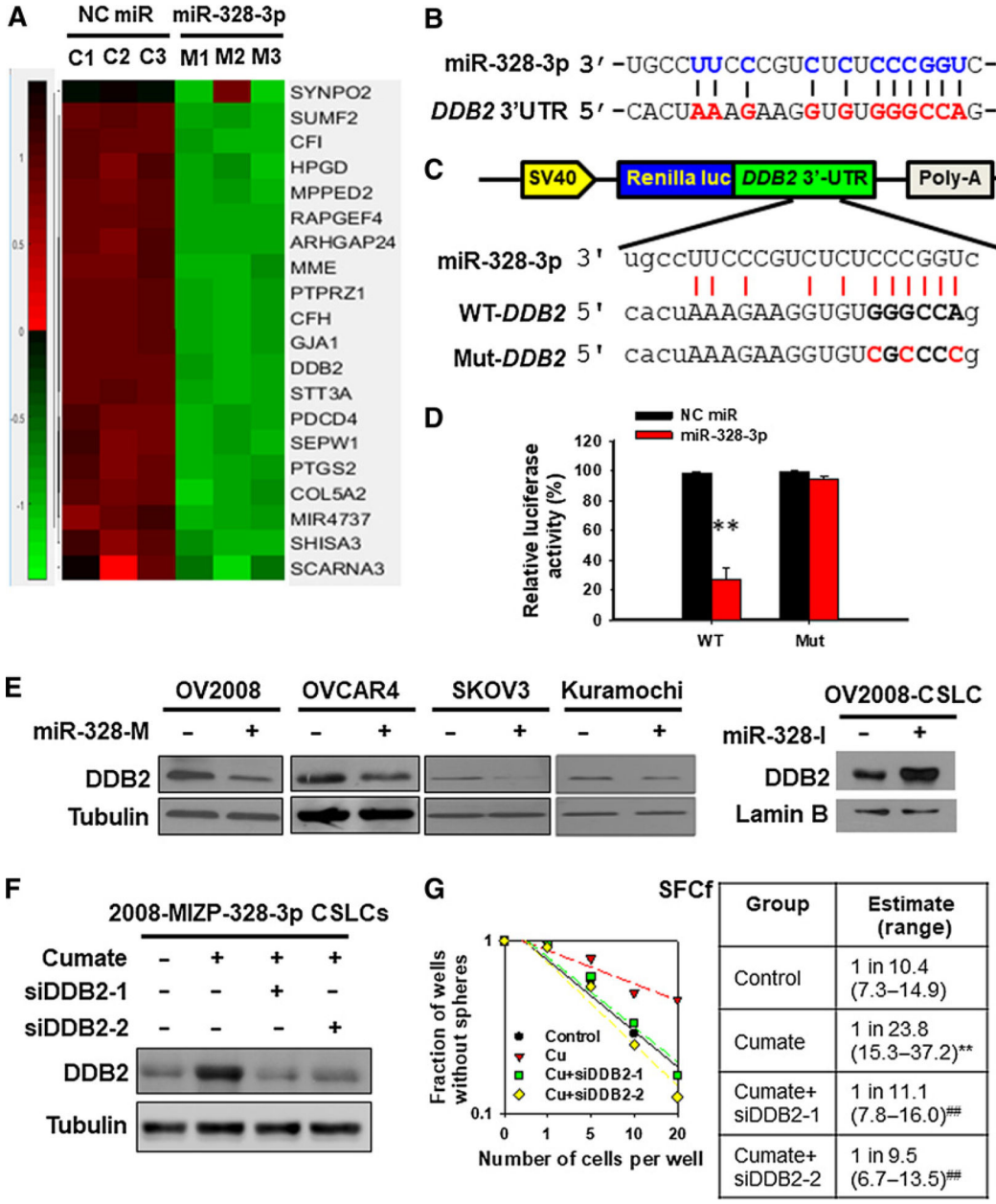

Group	Estimate (range)
Control	1 in 10.4 (7.3–14.9)
Cumate	1 in 23.8 (15.3–37.2)**
Cumate+ siDDB2-1	1 in 11.1 (7.8–16.0)##
Cumate+ siDDB2-2	1 in 9.5 (6.7–13.5)##

Figure 3.

DDB2 is a direct target of miR-328 and mediates the function of miR-328 in the regulation of CSC properties. **A,** Gene expression heatmap from microarray analysis of miR-328–overexpressing ovarian cancer cells. OV2008 cells were transfected with miR-328 mimics or NC miR for 2 days. Total RNA was isolated, and the differentially expressed genes were screened using GeneChip Human Transcriptome Array 2.0. **B,** Predicted binding of miR-328 to the 3′-UTR of *DDB2*. **C** and **D,** Dual luciferase reporter assay shows the interaction of miR-328 and its targeting sequence in the DDB2 3′-UTR. OV2008 cells were transfected with psiCHECK-2 containing the wild-type (WT) or mutated (Mut) target site of the *DDB2* 3′-UTR (**C**) plus miR-328-M or NC miR for 48 hours. The luciferase activity was determined and normalized to the Firefly activity and presented as relative activity to the

corresponding NC miR (**D**). $N = 3$; bar, SD; **, $P < 0.01$. **E,** miR-328 downregulates the DDB2 protein level. miR-328-M was transfected into various EOC cell lines for 48 hours, and miR-328-I was transfected into OV2008-CSLCs for 48 hours; immunoblotting analyses were conducted to show the protein level of DDB2 in these cells. **F** and **G,** DDB2 downregulation antagonizes anti-miR-328-reduced sphere formation capability of ovarian CSLCs. The 2008-MIZP328–3p cells were treated with cumate to induce miR-328 inhibition. Meanwhile, cells were also transfected with two different siDDB2 for 48 hours, and DDB2 expression was determined (**F**). Cells were plated in Ultra-Low Attachment 96-well plates in a limiting dilution manner, and the number of wells containing spheres was counted after 12 days to generate the SFCf (**G**). **, $P < 0.01$ compared with control; $^{\#\#}$, $P < 0.01$ compared with cumate.

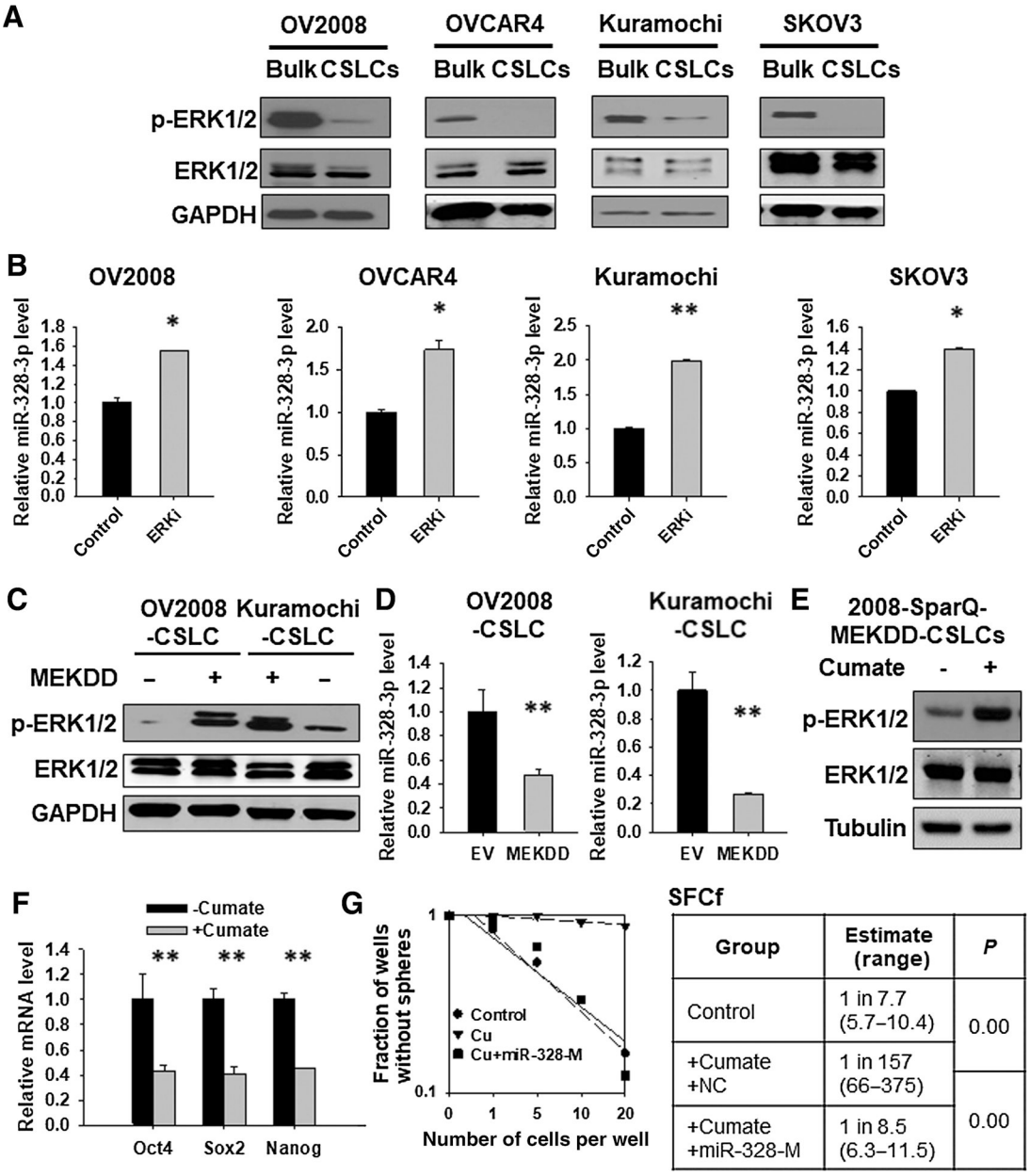

Group	Estimate (range)	*P*
Control	1 in 7.7 (5.7–10.4)	0.00
+Cumate +NC	1 in 157 (66–375)	
+Cumate +miR-328-M	1 in 8.5 (6.3–11.5)	0.00

Figure 4.

Reduced ERK signaling activity contributes to the upregulation of miR-328 expression and maintenance of CSC properties in ovarian CSLCs. **A,** Expression of p-ERK1/2 in CSLCs isolated from various ovarian cancer cell lines. Spheroid (CSLCs) and adherent (Bulk) cells were harvested from various EOC cell lines. p-ERK1/2 was determined using immunoblotting; ERK1/2 and GAPDH were also determined to serve as loading controls. **B,** Inhibition of the ERK signaling enhanced miR-328 expression. EOC cell lines were treated with the ERK inhibitor U0126 for 24 hours, RNA was isolated, and the miR-328 level was determined using qRT-PCR. $N = 3$; bar, SD; *, $P < 0.05$; **, $P < 0.01$. **C** and **D,** Activation of the ERK signaling reduced the expression of miR-328. OV2008 and Kuramochi CSLCs were transiently transfected with either empty vector or MEKDD expressing vector for 48

hours; immunoblotting was used to determine the expression of p-ERK1/2 (**C**), and qRT-PCR was used to determine the level of miR-328 (**D**). $N = 3$; bar, SD; **, $P < 0.01$. **E,** Cumate induced ERK1/2 phosphorylation in 2008-SparQ-MEKDD CSLCs. **F,** Activation of the ERK signaling by treating cells with cumate reduced the expression level of stem cell–specific genes in 2008-SparQ-MEKDD CSLCs. $N = 3$; bar, SD; **, $P < 0.01$. **G,** Overexpression of miR-328 antagonized the decrease of SFCf induced by ERK activation. The 2008-SparQ-MEKDD CSLCs were treated with or without cumate. Meanwhile, cells were transfected with miR-328-M. After 3 days, the SFCf was determined using the sphere formation assay in a limiting dilution manner.

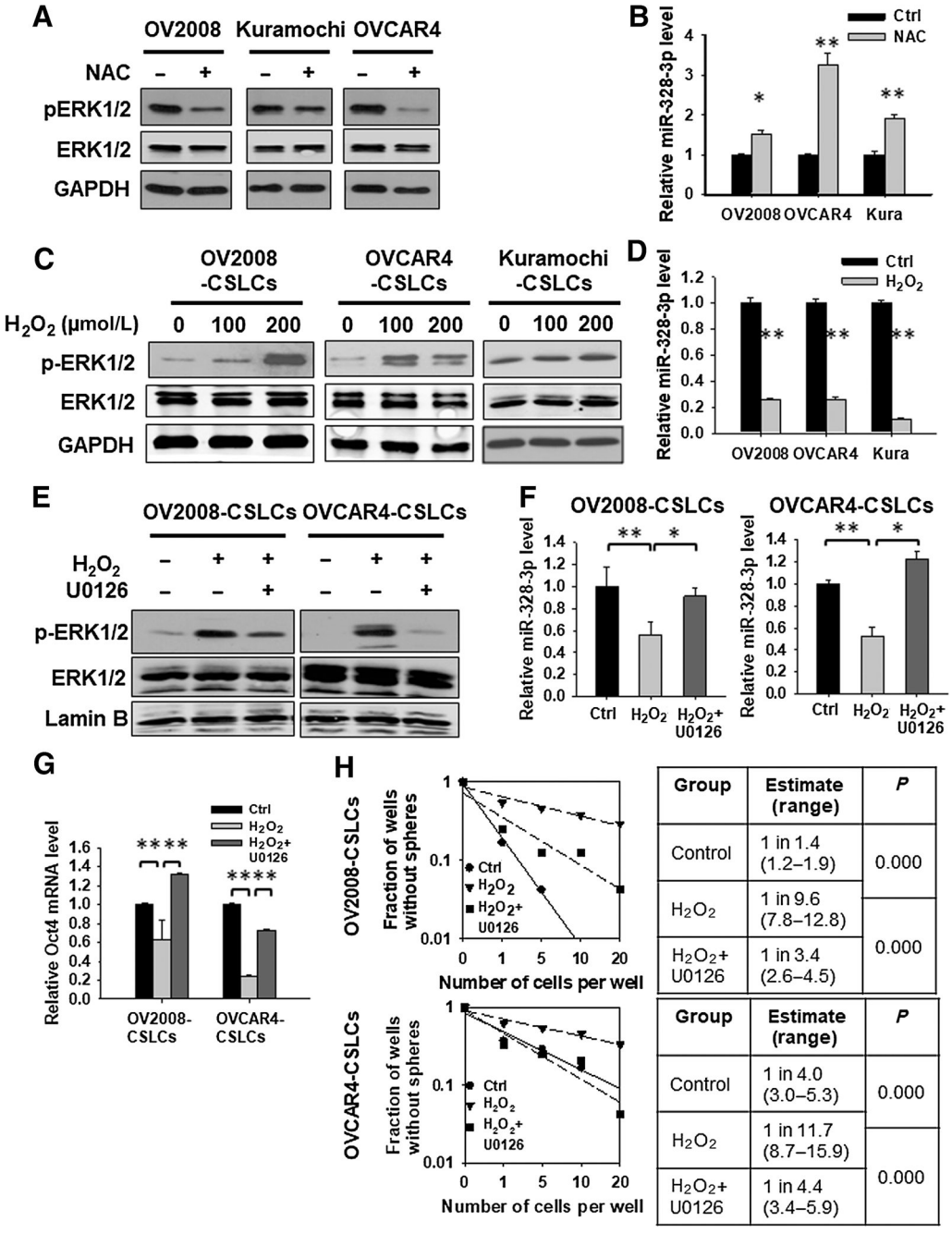

Group	Estimate (range)	P
Control	1 in 1.4 (1.2–1.9)	0.000
H_2O_2	1 in 9.6 (7.8–12.8)	0.000
H_2O_2+ U0126	1 in 3.4 (2.6–4.5)	

Group	Estimate (range)	P
Control	1 in 4.0 (3.0–5.3)	0.000
H_2O_2	1 in 11.7 (8.7–15.9)	0.000
H_2O_2+ U0126	1 in 4.4 (3.4–5.9)	

Figure 5.

Low ROS level contributes to the reduced ERK activity and enhanced miR-328 expression in ovarian CSLCs. **A** and **B,** Depleting ROS inhibits the ERK1/2 phosphorylation and increases miR-328 expression in ovarian cancer cell lines. Various EOC cell lines were treated with the ROS inhibitor N-acetyl-L-cysteine (NAC, 10 mmol/L) for 12 hours, p-ERK1/2 was detected using Western blotting (**A**), and miR-328 expression was determined using qRT-PCR (**B**). $N = 3$; bar, SD; *, $P < 0.05$; **, $P < 0.01$. **C** and **D,** Oxidative stress enhances ERK phosphorylation and reduces miR-328 expression in ovarian CSLCs. CSLCs enriched from various EOC cell lines were treated with H_2O_2 for 24 hours. p-ERK1/2 was

detected using Western blotting (**C**), and miR-328 expression was determined using qRT-PCR (**D**). $N = 3$; bar, SD; **, $P < 0.01$. **E–H,** ERK signaling inhibition antagonizes H_2O_2-induced reduction of miR-328 expression and CSC properties. OV2008-CSLCs and OVCAR4-CSLCs were treated with H_2O_2 and/or the ERK inhibitor U0126 for 24 hours, and the p-ERK1/2 level was determined using immunoblotting (**E**). **F,** The miR-328 level was determined using qRT-PCR. $N = 3$; bar, SD; *, $P < 0.05$; **, $P < 0.01$. **G,** Expression of the stem cell–specific gene *Oct4* was determined using qRT-PCR. $N = 3$; bar, SD; **, $P < 0.01$. The SFCf in these cells were determined using the sphere formation assay with limiting dilution (**H**).

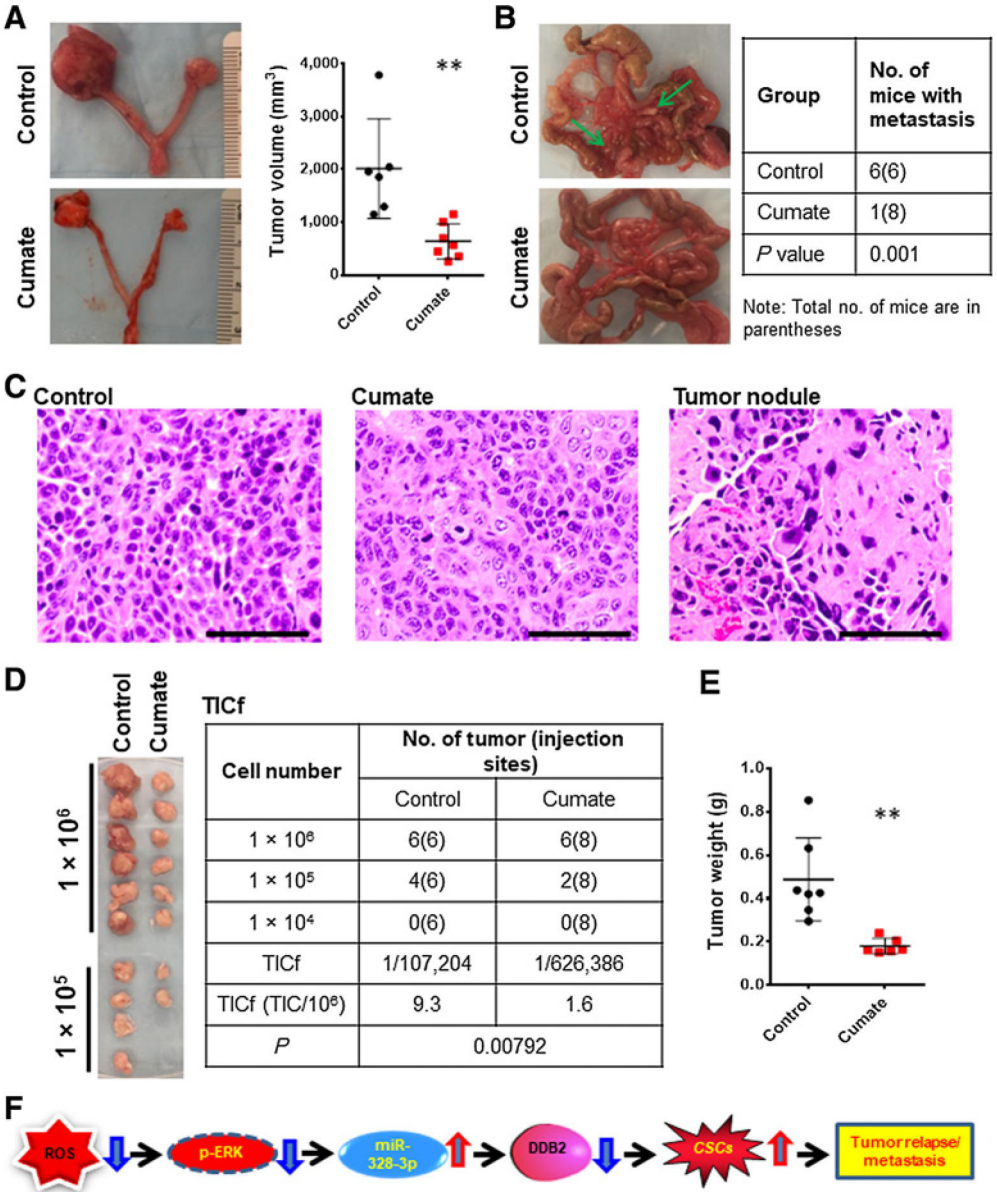

Figure 6.

Inhibition of miR-328 impedes tumor growth and metastasis in the orthotopic ovarian xenograft model. **A,** Representative images of orthotopic ovarian xenografts generated by injecting 2008-MIZP328–3p cells into the ovary of nude mice. Volumes of xenografts in mice treated or untreated with cumate were measured. **, $P < 0.01$. **B,** Macroscopic appearances and counts of ovarian metastasis nodules in peritoneal cavity. **C,** Representative H&E-stained images of the xenograft tumors and metastasis nodules. Bar, 100 μm. **D** and **E,** Xenotransplantation limiting dilution assay was used to estimate TICs in these xenografts. Tumor cells were isolated from xenografts and injected into NOD/SCID mice subcutaneously in a limiting dilution manner. Images of tumors after 2 weeks of injection were presented, and the number of xenografts was counted to generate TICf using the online algorithm described in Materials and Methods (**D**). Weight of tumors generated with 1×10^6

xenograft cells isolated from control and cumate-treated mice bearing orthotopic xenografts (**E**). **F**, Model of the mechanism by which miR-328 regulates the maintenance of CSC properties and tumor metastasis.